Article ID: 0253-2778(2008)03-0306-08

An enhanced meshfree treatment for symmetric/antisymmetric and periodic problems

WANG Dong-dong

(*Department of Civil Engineering, Xiamen University, Xiamen*, 361005 *China*)

Abstract: Most of the existing meshfree methods are based on moving least square (MLS) or reproducing kernel (RK) approximation. One noticeable property of the MLS/RK approximation is the boundary truncation effect. An enhanced treatment of the special conditions of symmetry, antisymmetry and periodicity in meshfree methods was proposed such that the reduced model was able to yield identical solutions as the full model. In the proposed method, the exterior nodes (dummy nodes) beyond the partial model (discretized with physical nodes) were included into the construction of MLS/RK approximation. Furthermore, using the kinematic relationship the extra dummy nodes were linked to those physical nodes on the partial problem domain being modeled and thus no additional degrees of freedom came into the later computation. It is shown that with this straightforward modification, the resulting meshfree approximation based on the partial model is exactly equivalent to that constructed from the full model. Then the truncation effect is totally removed. The superior performance of the proposed approach compared to the original meshfree formulation is verified through several symmetric, antisymmetric and periodic examples. A possible strategy for removing general boundary effect was also presented.

Key words: meshfree methods; symmetry/antisymmetry and periodicity; boundary truncation effect; dummy nodes

CLC number: O242.21 **Document code**: A

一种计算对称反对称及周期性问题的改进无网格法

王东东

(厦门大学土木工程系,福建厦门 361005)

摘要:分析对称反对称或周期性问题时,通常只需要取一半或一个周期的局部模型进行离散求解.由于无网格法存在较为显著的边界截断效应,与整体模型相比局部模型的无网格解答精度会有所下降,在边界附近更为显著.为消除这种边界效应,提出了一种改进的无网格近似方法.该方法考虑了局部模型外的节点(虚拟节点)对于模型内各节点(真实节点)的近似影响,并利用对称反对称或周期性关系压缩虚拟节点的自由度,在不增加额外自由度的条件下能够使局部模型和整体模型得到完全相同的结果.通过求解对称反对称和周期

Received: 2006-12-15; **Revised**: 2007-11-08

Foundation item: NSFC(10602049).

Biography: WANG Dong-dong (corresponding author), male, PhD/Associate Professor. E-mail: ddwang@xmu.edu.cn

性问题算例验证了该方法的有效性. 最后对一般性问题的无网格边界效应也进行了简要的讨论.
关键词:无网格法;对称反对称及周期性问题;边界截断效应;虚拟节点

0 Introduction

Typical conditions such as symmetry, antisymmetry and periodicity often occur for a large class of engineering problems. Commonly we can utilize these special characteristics to simplify the computation by only modeling part of the problems, i. e., half model for symmetric or antisymmetric cases, unit cell for periodic problems. Since the 1980's the so-called meshfree methods have been very actively developed and applied to solving various engineering and scientific problems[1~6]. Most of these methods are based on moving least square (MLS) or reproducing kernel (RK) approximation[1~3]. With monomial basis functions these two methods give an identical approximation. One major difference between the MLS/RK approximation and the conventional finite element approximation is that the MLS/RK approximation generally is not an interpolation function. Moreover, the shape functions associated with the nodes right at or near the boundary are not the same as those related to the interior nodes, which exhibits a boundary truncation phenomenon or boundary effect whereas there are no such problems for finite elements. As we know, the interior parts become new boundaries when the symmetric, antisymmetric or periodic conditions are invoked. Thus after meshfree discretization and analysis based on the partial model, due to the boundary truncation effect the results won't be the same as those obtained from full model simulation.

In this paper, an enhanced meshfree approximation strategy is presented to eliminate this boundary cut-off effect mentioned above. In this method, the exterior nodes (dummy nodes) beyond the partial model (discretized with physical nodes) are included into the construction of MLS/RK approximation. Furthermore, based on the kinematic relationship the extra dummy nodes are cross-linked to their corresponding physical nodes. In this way no additional degrees of freedom are added to the later computation. It is shown that with this straightforward modification, the resulting meshfree approximation based on the partial model is identical to that based upon the full model, then the truncation effect is totally removed. The present approximation yields identical results as the full model solutions, obviously with much less computational cost. The superior performance of the proposed approach compared to the original meshfree formulation is verified through several symmetric, antisymmetric and periodic examples. The boundary effect for general problems is also discussed and a method is proposed as well to improve the solution accuracy. It is noted that the imaginary or ghost node approach was also proposed in the collocated SPH to apply the boundary conditions[7]. Compared with SPH the realistic boundary conditions can be implemented more easily for the MLS/RK based Galerkin meshfree formulations, and there are several effective methods such as Lagrangian multiplier method, coupled meshfree and FE method, transformation method, etc[3,4]. The mixed transform method is employed here to efficiently enforce the boundary conditions. It should be pointed out that the focus of this work is not to impose boundary conditions but to use auxiliary dummy nodes to construct a more uniform approximation for better solution accuracy in solving problems involving symmetry/antisymmetry and periodicity.

1 MLS/RK approximation

In this section the MLS/RK approximation is summarized. For convenience in expression, the following multi-index notations are used, i. e

$$\left.\begin{aligned}&\boldsymbol{\alpha}\equiv(\alpha_1\cdots\alpha_{n_{sd}});\ \boldsymbol{\alpha}!\equiv\alpha_1!\cdots\alpha_{n_{sd}}!;\\&(\boldsymbol{x}-\boldsymbol{x}_I)^{\boldsymbol{\alpha}}\equiv(x_1-x_{I1})^{\alpha_1}\cdots(x_{n_{sd}}-x_{In_{sd}})^{\alpha_{n_{sd}}}\\&|\boldsymbol{\alpha}|\equiv\alpha_1+\cdots+\alpha_{n_{sd}};\\&D^{\boldsymbol{\alpha}}[u(\boldsymbol{x})]\equiv\partial^{|\boldsymbol{\alpha}|}u(\boldsymbol{x})/\partial\boldsymbol{x}^{\boldsymbol{\alpha}}=\\&\qquad\partial^{|\boldsymbol{\alpha}|}u(\boldsymbol{x})/\partial x_1^{\alpha_1}\cdots\partial x_{n_{sd}}^{\alpha_{n_{sd}}}\end{aligned}\right\}\tag{1}$$

where n_{sd} denotes the dimensions of space. Consider a domain Ω discretized by a set of NP particles $x_I, I=1,2,\cdots,\mathrm{NP}$, the approximation of a variable $u(x)$, denoted by $u^h(x)$ can be expressed as

$$u^h(x)=\sum_{I=1}^{\mathrm{NP}}\Psi_I(x)d_I\tag{2}$$

where Ψ_I and d_I are the shape function and nodal parameter associated with node I. If the n_{th} order monomial basis is used, Ψ_I takes the following form

$$\Psi_I(\boldsymbol{x})=\boldsymbol{H}^{\mathrm{T}}(\boldsymbol{x}-\boldsymbol{x}_I)\boldsymbol{b}(\boldsymbol{x})\boldsymbol{\phi}_{a_I}(\boldsymbol{x}-\boldsymbol{x}_I)\tag{3}$$

where $\boldsymbol{H}^{\mathrm{T}}(\boldsymbol{x}-\boldsymbol{x}_I)$ is the basis vector defined as

$$\begin{aligned}&\boldsymbol{H}^{\mathrm{T}}(\boldsymbol{x}-\boldsymbol{x}_I)=[(\boldsymbol{x}-\boldsymbol{x}_I)^{\boldsymbol{\alpha}}]_{|\boldsymbol{\alpha}|\leqslant n}=\\&\quad[1\quad x_1-x_{I1}\quad\cdots\quad(x_{n_{sd}}-x_{In_{sd}})^2\quad(x_1-x_{I1})^2\\&\quad\cdots\quad(x_{n_{sd}}-x_{In_{sd}})^n]\end{aligned}\tag{4}$$

and the coefficient vector $\boldsymbol{b}(x)$ is

$$\begin{aligned}&\boldsymbol{b}^{\mathrm{T}}(\boldsymbol{x})=[b_\alpha(\boldsymbol{x})]_{|\boldsymbol{\alpha}|\leqslant n}=\\&\quad[b_{0\cdots0}(\boldsymbol{x})\quad b_{10\cdots0}(\boldsymbol{x})\quad\cdots\quad b_{0\cdots01}(\boldsymbol{x})\quad b_{20\cdots0}(\boldsymbol{x})\\&\quad\cdots\quad b_{0\cdots0n}(\boldsymbol{x})]\end{aligned}\tag{5}$$

The function $\boldsymbol{\phi}_{a_I}(\boldsymbol{x}-\boldsymbol{x}_I)$ is called kernel function which centers at x_I and has a compact support $\boldsymbol{a}_I$. The typical cubic spline[3] is used in this study and the 2D funcation is constructed as a tensor product of two 1D splines.

The coefficient vector $\boldsymbol{b}(x)$ is obtained via imposing up to n_{th} order consistency conditions

$$\left.\begin{aligned}&\sum_{I=1}^{\mathrm{NP}}\Psi_I(\boldsymbol{x})\boldsymbol{x}_I^{\boldsymbol{\alpha}}=\boldsymbol{x}^{\boldsymbol{\alpha}}\\\text{or}\quad&\sum_{I=1}^{\mathrm{NP}}\Psi_I(\boldsymbol{x})(\boldsymbol{x}-\boldsymbol{x}_I)^{\boldsymbol{\alpha}}=\boldsymbol{\delta}_{|\boldsymbol{\alpha}|0},\ |\boldsymbol{\alpha}|\leqslant n\end{aligned}\right\}\tag{6}$$

Eq. (6) can be rewritten as a matrix form as

$$\sum_{I=1}^{\mathrm{NP}}\Psi_I(\boldsymbol{x})\boldsymbol{H}(\boldsymbol{x}-\boldsymbol{x}_I)=\boldsymbol{H}(\boldsymbol{0})\tag{7}$$

Substituting Eq. (3) into Eq. (7) yields

$$\left.\begin{aligned}&\boldsymbol{b}(\boldsymbol{x})=\boldsymbol{M}^{-1}(\boldsymbol{x})\boldsymbol{H}(\boldsymbol{0})\\&\boldsymbol{M}(\boldsymbol{x})\equiv\sum_{I=1}^{\mathrm{NP}}\boldsymbol{H}(\boldsymbol{x}-\boldsymbol{x}_I)\boldsymbol{H}^{\mathrm{T}}(\boldsymbol{x}-\boldsymbol{x}_I)\boldsymbol{\phi}_{a_I}(\boldsymbol{x}-\boldsymbol{x}_I)\end{aligned}\right\}\tag{8}$$

Finally the meshfree shape function is obtained as

$$\Psi_I(\boldsymbol{x})=\boldsymbol{H}^{\mathrm{T}}(\boldsymbol{0})\boldsymbol{M}^{-1}(\boldsymbol{x})\boldsymbol{H}(\boldsymbol{x}-\boldsymbol{x}_I)\boldsymbol{\phi}_{a_I}(\boldsymbol{x}-\boldsymbol{x}_I)\tag{9}$$

From the consistency condition we have the relationship for the derivatives of shape function

$$\left.\begin{aligned}&\sum_{I=1}^{\mathrm{NP}}D^{\boldsymbol{\alpha}}[\Psi_I(\boldsymbol{x})]\boldsymbol{x}_I^{\boldsymbol{\beta}}=[\boldsymbol{\beta}!/(\boldsymbol{\beta}-\boldsymbol{\alpha})!]\boldsymbol{x}^{(\boldsymbol{\beta}-\boldsymbol{\alpha})}\\\text{or}\quad&\sum_{I=1}^{\mathrm{NP}}D^{\boldsymbol{\alpha}}[\Psi_I(\boldsymbol{x})](\boldsymbol{x}_I-\boldsymbol{x})^{\boldsymbol{\beta}}=\boldsymbol{\alpha}!\boldsymbol{\delta}_{\boldsymbol{\alpha}\boldsymbol{\beta}}\\&\qquad|\boldsymbol{\alpha}|\leqslant n,\ |\boldsymbol{\beta}|\leqslant n\end{aligned}\right\}\tag{10}$$

where $\boldsymbol{\delta}_{\boldsymbol{\alpha}\boldsymbol{\beta}}\equiv\delta_{\alpha_1\beta_1}\delta_{\alpha_2\beta_2}\cdots\delta_{\alpha_{n_{sd}}\beta_{n_{sd}}}$.

2 Motivation

Consider the following 1D boundary value problem

$$\left.\begin{aligned}&u_{,xx}+2(\mathrm{sech}(2x))^2=0,\ x\in(-2,2)\\&u(-2)=0,\ u(2)=0\end{aligned}\right\}\tag{11}$$

The exact solution of this problem is given by

$$\left.\begin{aligned}&u(x)=\{\log[\cosh(4)]-\log[\cosh(x)]\}/2\\&u_{,x}(x)=-\tanh(2x)\end{aligned}\right\}\tag{12}$$

Note $u(x)$ and $u_{,x}(x)$ are symmetric and antisymmetric respectively about $x=0$. Due to the symmetry, we can solve the problem using a half model discretization with symmetric boundary condition $u_{,x}=0$ prescribed at $x=0$. Here 6 uniform distributed nodes and a normalized support size 2 are used to solve the half model problem and Fig. 1(b) shows the gradient solution. For comparison this problem is solved again using 11 equally spaced nodes with normalized support size 2 by the full model and the result is shown in Fig. 1(a). A comparison of both results indicates that full and half models yield unexpected different numerical solutions.

This unexpected difference is due to the

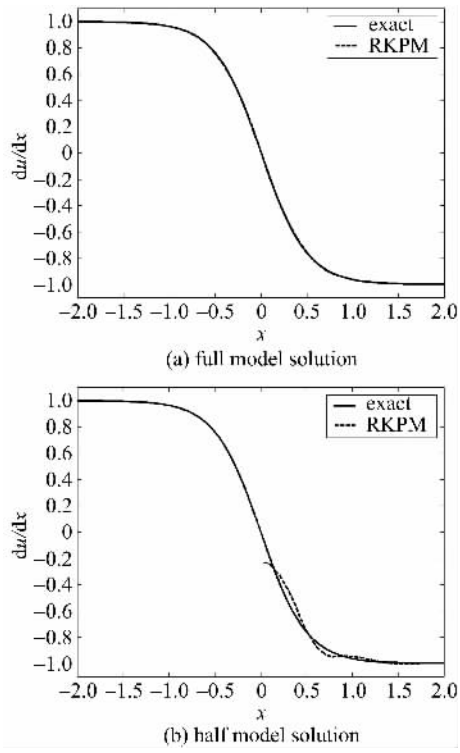

Fig. 1 Gradient solution comparison of 1D symmetric problem

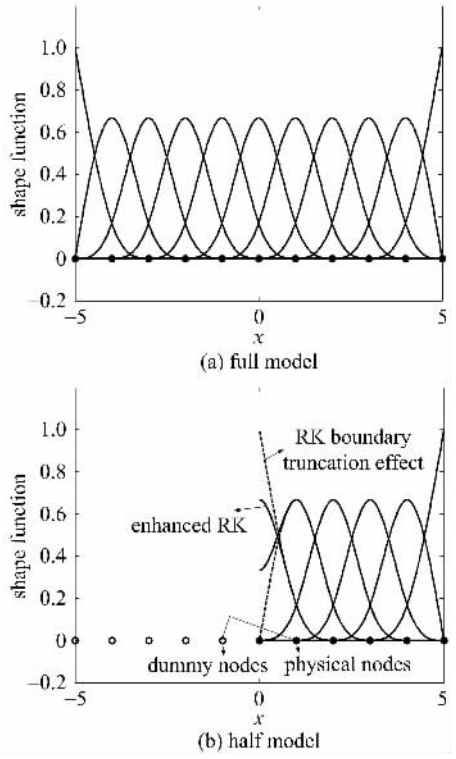

Fig. 2 Comparison of meshfree shape functions

meshfree approximation functions. Here we use a 1D case to illustrate the details. Fig. 2(a) shows the 1D meshfree shape functions based on an 11-node uniform discretization. It is clear that unlike FEM, for MLS/RK approximation even a uniform nodal distribution gives non-uniform shape functions over the problem domain, especially close to the boundary, here we refer to this as the boundary truncation effect. When dealing with the half model, actually a new boundary is created at the symmetric interface and thus due to the boundary truncation effect the meshfree approximation field using the half model is not equivalent to that of the full model as shown in Fig. 2(b), where the dash lines represents the half model shape functions. Then a conventional symmetric treatment fails to reproduce the full model results and leads to a reduction of solution accuracy.

3 Enhanced treatment of symmetric/antisymmetric problems

To get a half model solution equivalent to that of the full model this truncation effect needs to be eliminated. A systematic procedure is proposed for the elimination of boundary truncation effect. Without loss of generality, let's first consider a 1D symmetric problem to illustrate the proposed approach.

To achieve symmetry in meshfree approximation, as shown in Fig. 3, the additional symmetric exterior nodes (dummy nodes) beyond the half model are included in the construction of MLS/RK approximation. Since the field variables are also symmetric, these added nodes share the same nodal values as their corresponding particles (physical nodes) in the half domain being modeled. Imposing this kinematic symmetry and using static condensation, these additional nodes can be eliminated so that no new degrees of freedom are introduced. Thus the enhanced meshfree approximation is given as

$$\left.\begin{aligned} u^h(\boldsymbol{x}) &= \sum_I^{\mathrm{NP}} \overline{\Psi}_I(\boldsymbol{x}) d_I \\ \overline{\Psi}_I(\boldsymbol{x}) &= \begin{cases} \Psi_{I^-}(\boldsymbol{x}) + \Psi_{I^+}(\boldsymbol{x}), & \Gamma^s \in \mathrm{supp}(I) \\ \Psi_I(\boldsymbol{x}), & \Gamma^s \notin \mathrm{supp}(I) \end{cases} \end{aligned}\right\} \tag{13}$$

where Γ^s represents the symmetric interface.

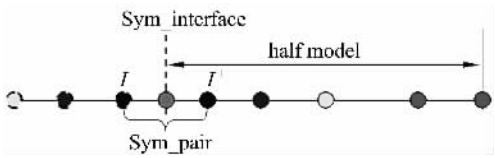

Fig. 3 1D discretization for symmetric problems

These new condensed shape functions are shown in Fig. 2(b) where clearly no boundary truncation effect occurs. Note here the problem is still formulated on the half domain which is much more computationally efficient than modeling of the whole problem. With this enhanced MLS/RK approximation, the symmetric problem of Eq. (11) is recalculated and the result is shown in Fig. 4. It is observed that based on this enhanced approximation, the solution with the half model is exactly identical to that of the full model result. As shown in Fig. 5, this approach can be easily extended to 2D or 3D problems by defining $\overline{\Psi}_I(\boldsymbol{x})$ as

$$\overline{\Psi}_I(\boldsymbol{x}) = \begin{cases} \sum_{J\in IP} \Psi_J(\boldsymbol{x}), & \Gamma^s \in \text{supp}(I) \\ \Psi_I(\boldsymbol{x}), & \Gamma^s \notin \text{supp}(I) \end{cases} \tag{14}$$

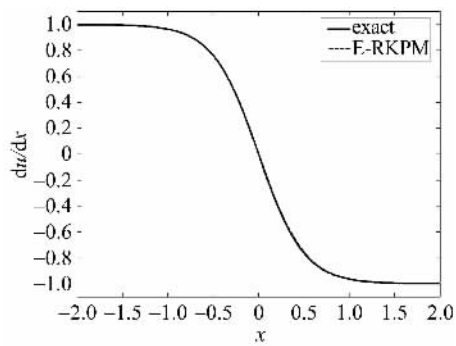

Fig. 4 Half model gradient solution with the enhanced RK approximation

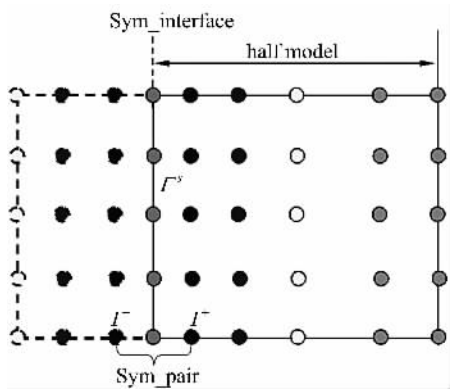

Fig. 5 2D discretization for symmetric problems

where IP represents a symmetric meshfree particle pair associated with node I whose support covers the symmetric boundary Γ^s.

4 Extension to periodic problems

4.1 Periodic MLS/RK approximation

Periodicity is another special case often encountered in numerical analysis. One typical engineering application is the periodic boundary conditions usually imposed in computational homogenization[8]. As shown in Figs. 6 and 7 periodicity implies infinity of repeated domains and periodic conditions over a period $\boldsymbol{\Sigma}$, such as

$$u(\boldsymbol{x}) = u(\boldsymbol{x} + i\boldsymbol{\Sigma}),\ i = \pm 1, \pm 2, \pm 3, \cdots \tag{15}$$

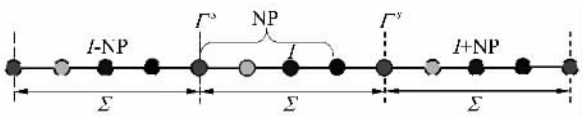

Fig. 6 1D discretization for periodic problems

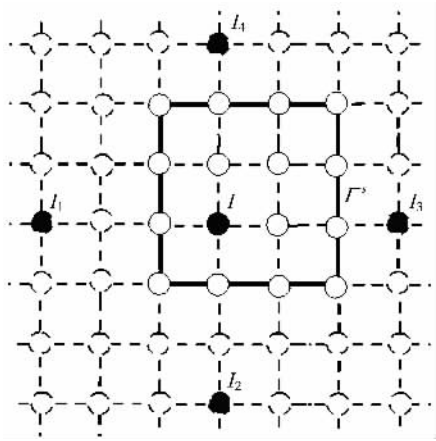

Fig. 7 2D discretization for periodic problems

Due to periodicity only one of these repeated domains, called unit cell, needs to be considered. However similar to the symmetry we discussed, the MLS/RK shape functions can not give a fully periodic operator within one of the periodic domains. Similar to the enhanced treatment for symmetry, the periodicity in meshfree formulation can be achieved by including extra periodic exterior nodes outside the unit cell being considered. Taking the advantage of periodicity, the degrees of freedom associated with the additional nodes can be removed such as the problem is formulated only

with the degrees of freedom related to physical nodes within the unit cell. For the particle distribution shown in Fig. 6, the enhanced periodic approximation is expressed as

$$\left.\begin{aligned} u^h(\boldsymbol{x}) &= \sum_I \overline{\Psi}_I(\boldsymbol{x}) d_I \\ \overline{\Psi}_I(\boldsymbol{x}) &= \begin{cases} \Psi_I(\boldsymbol{x}) + \Psi_{I+\mathrm{NP}}(\boldsymbol{x}) + \Psi_{I-\mathrm{NP}}(\boldsymbol{x}), & \\ \qquad\qquad \Gamma^s \in \mathrm{supp}(I) & \\ \Psi_I(\boldsymbol{x}), \quad \Gamma^s \notin \mathrm{supp}(I) & \end{cases} \end{aligned}\right\} \tag{16}$$

In 2D case, for the a repeated structure of unit cells as shown in Fig. 7, only the cell with a solid boundary is modeled where the exterior nodes are present only for the purpose of approximation. The enhanced meshfree shape function has the same form of Eq. (14), where IP denotes a set of particles associated with the physical node I whose support covers the periodic boundary Γ^s, which is formed by particles with repeated period from node I, i. e., in Fig. 7 $IP=\{I, I_1, I_2, I_3, I_4\}$.

4.2 Numerical verification

Consider the following 2D example with periodic response

$$\left.\begin{aligned} -\Delta u &= 32\pi^2 \sin(4\pi x)\sin(4\pi y) \quad \text{in} \quad \Omega \\ u(x) &= 0 \quad \text{on} \quad \partial\Omega \end{aligned}\right\} \tag{17}$$

where Δ is the Laplacian operator and Ω denotes a square domain with a unit length. As shown in Fig. 8 the exact solution to this problem is given by

$$u(x,y) = \sin(4\pi x)\sin(4\pi y) \tag{18}$$

This problem is solved by a 7×7 uniformly spaced meshfree particles and the normalized support size is set to be 2. The numerical solutions by both conventional and enhanced meshfree formulations are shown in Fig. 9, where the higher accuracy of the enhanced meshfree approximation solution is obviously demonstrated.

5 Possible remedy to general boundary truncation effect

In the above, we mainly concentrate on three special boundary conditions commonly appearing in engineering problems. For general bounded problems the boundaries are unavoidable and the

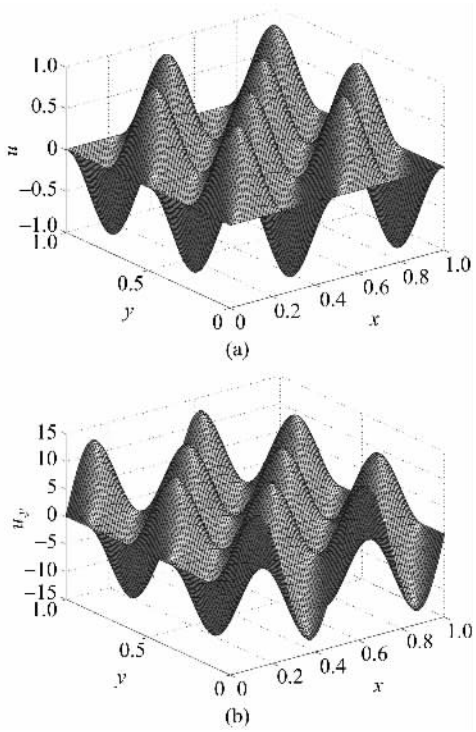

Fig. 8　Exact solutions of u and $u_{,y}$ for the 2D periodic problem

boundary truncation shortcoming always exists. Consider the following one dimensional elasticity problem

$$\left.\begin{aligned} &(EAu_{,x})_{,x} + b(x) = 0,\ x \in (0,10) \\ &u(0) = 0, \quad u(10) = 1 \\ &b(x) = -100x + 1\,000x^2 - 150x^3,\ EA = 10\,000 \end{aligned}\right\} \tag{19}$$

This problem is solved by RKPM using 11 and 21 uniform nodes with a normalized support size of 2. The strain results are shown in Fig. 10. It can be seen that even with 21 meshfree nodes the numerical error is quite evident, close to the right boundary which is a high gradient region. So the model refinement does not effectively reduce the solution error.

Motivated by the previous enhancement with exterior nodes, we believe that one way to remove the boundary effect is to add extra nodes lying outside the problem domain. As shown in Fig. 11 the procedure is very straightforward. The problem domain is discretized by a set of nodes with solid circles, and some exterior nodes denoted

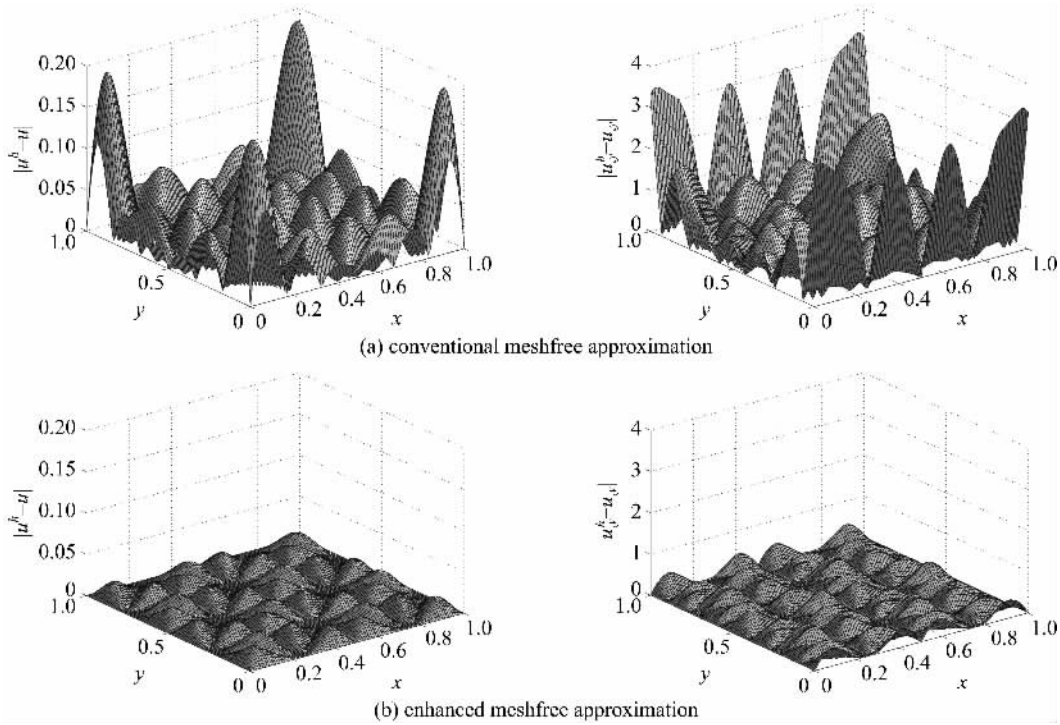

Fig. 9 Comparison of u^h and $u^h_{,y}$

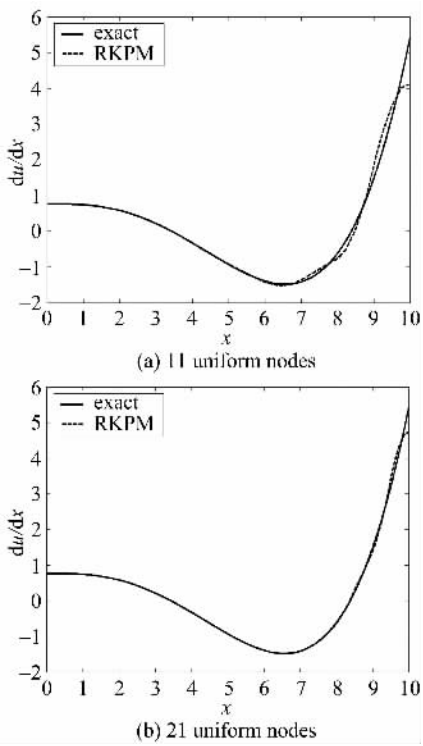

Fig. 10 Strain solution of Eq. (19)

by dash circles are also added to construct the meshfree approximation. Note that the weak form is still formulated and integrated on the real problem domain. By adding two uniform exterior

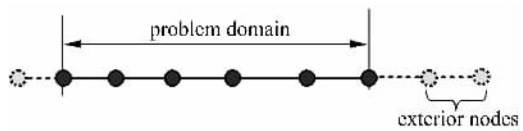

Fig. 11 Meshfree discretization with exterior nodes

nodes at the right boundary, the given problem is solved again using 11 equally spaced nodes. The result, as shown in Fig. 12(a), shows that by only including two nodes outside the boundary to build the approximation, the result is improved tremendously and matches the exact solution, even better than that of 21 nodes. An interesting comparison is that if an equal number of nodes, all the 13 nodes, are put within the problem domain, the solution accuracy is much lower as shown in Fig. 12(b). Then it is reasonable to say that the exterior nodes contribute significantly to accuracy improvement by reducing the boundary truncation effect in meshfree methods.

6 Conclusion

An enhanced treatment for symmetry, antisymmetry and periodicity in meshfree methods was proposed. In the present approach, the

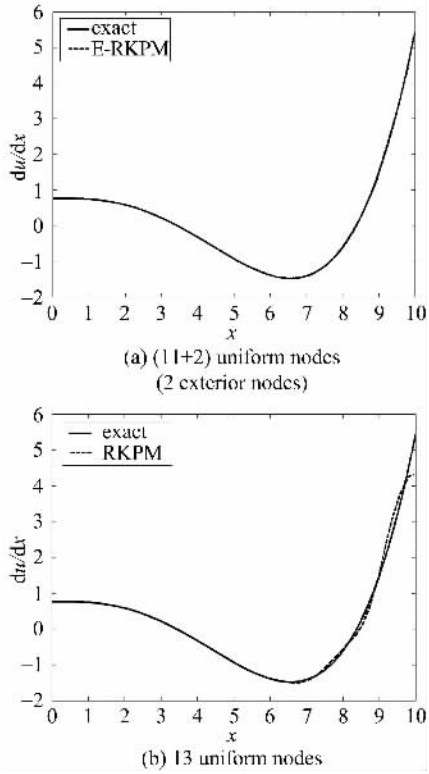

Fig. 12 Strain solution comparison of Eq. (19)

exterior nodes beyond the partial model are included to eliminate the boundary cut-off effect and construct the MLS/RK approximation. Moreover, these extra nodes are linked to those physical nodes on the partial problem model through their corresponding kinematic relationship. Thus the proposed approach does not entail additional degrees of freedom for the whole computation. It was shown that with the straightforward enhancement, the partial model solution is equivalent to that using the full model. The superior performance of the proposed approach compared to the original meshfree formulation was demonstrated through several numerical examples. A possible remedy for general boundary truncation effect was also presented via a numerical example.

References

[1] Belytschko T, Lu Y Y, Gu L. Element-free Galerkin methods [J]. International Journal for Numerical Methods in Engineering, 1994, 37(2): 229-256.

[2] Liu W K, Jun S, Zhang Y F. Reproducing kernel particle methods [J]. International Journal for Numerical Methods in Fluids, 1995, 20(8-9): 1 081-1 106.

[3] Chen J S, Pan C H, Wu C T, et al. Reproducing kernel particle methods for large deformation analysis of non-linear structures [J]. Computer Method in Applied Mechanics and Engineering, 1996, 139(1): 195-227.

[4] Belytschko T, Kronggauz Y, Organ D, et al. Meshless methods: an overview and recent developments [J]. Computer Method in Applied Mechanics and Engineering, 1996, 139(1): 3-47.

[5] Wang D D. Hybrid meshfree formulation for solids and structures [D]. Ph. D. Dissertation, University of California, 2003.

[6] Li S F, Liu W K. Meshfree Particle Methods [M]. Berlin, Heidelberg: Springer-Verlag, 2004.

[7] Randles P W, Libersky L D. Smoothed particle hydrodynamics: some recent improvements and applications [J]. Computer Method in Applied Mechanics and Engineering, 1996, 139(1): 375-408.

[8] Wang D D, Chen J S, Sun L Z. Homogenization of magnetostrictive particle-filled elastomers using an interface-enriched reproducing kernel particle method [J]. Finite Elements in Analysis and Design, 2003, 39(8): 765-782.